# PET with *O*-(2-$^{18}$F-Fluoroethyl)-L-Tyrosine in Peripheral Tumors: First Clinical Results

Dirk Pauleit, MD[1,2]; Gabriele Stoffels, MD[2]; Winfried Schaden, MD[2]; Kurt Hamacher, PhD[3]; Dagmar Bauer, PhD[2]; Lutz Tellmann, BS[2]; Hans Herzog, PhD[2]; Stefan Bröer, PhD[4]; Heinz H. Coenen, PhD[3]; and Karl-Josef Langen, MD[2]

[1]*Clinic of Nuclear Medicine, Heinrich-Heine-University Düsseldorf, Düsseldorf, Germany;* [2]*Brain Imaging Center West, Institute of Medicine, Research Center Jülich, Jülich, Germany;* [3]*Institute of Nuclear Chemistry, Research Center Jülich, Jülich, Germany; and* [4]*School of Biochemistry and Molecular Biology, Faculty of Science, Australian National University, Canberra, Australia*

*O*-(2-$^{18}$F-Fluoroethyl)-L-Tyrosine ($^{18}$F-FET) PET has shown promising results in brain tumor diagnosis. The aim of this prospective study was to evaluate $^{18}$F-FET PET in comparison with $^{18}$F-FDG PET in patients with peripheral tumors. **Methods:** Forty-four consecutive patients with suspected malignant tumors underwent $^{18}$F-FET PET and $^{18}$F-FDG PET within 7 d. Whole-body PET studies were performed 1 h after intravenous injection of 370 MBq of $^{18}$F-FET or $^{18}$F-FDG. Six patients were excluded from the analysis because a malignant tumor could not be verified. In 38 patients (7 with colorectal cancer, 6 with pancreatic cancer, 9 with head–neck cancer, 4 with lymphomas, 3 with lung cancer, 3 with ovarian cancer, 4 with breast cancer, and 2 with prostatic cancer), $^{18}$F-FET PET and $^{18}$F-FDG PET were compared. **Results:** $^{18}$F-FET was positive in only 13 of 38 patients (8 with head–neck cancer, 3 with breast cancer, and 2 with lung cancer), whereas $^{18}$F-FDG exhibited increased uptake in 37 of 38 patients. All squamous cell carcinomas were found to be $^{18}$F-FET–positive tumors (8 head–neck cancer and 2 lung cancer), whereas most adenocarcinomas were found to be $^{18}$F-FET–negative tumors. In patients with colorectal cancer, pancreatic cancer, ovarian cancer, prostatic cancer, and lymphomas, no increased $^{18}$F-FET uptake could be identified. All lesions that exhibited increased $^{18}$F-FET uptake also showed increased $^{18}$F-FDG uptake. No additional lesion was identified by $^{18}$F-FET PET but not by $^{18}$F-FDG PET. A subgroup analysis of patients with head–neck carcinomas allowed a better distinction between malignant and inflammatory tissues with $^{18}$F-FET than with $^{18}$F-FDG. **Conclusion:** $^{18}$F-FET is inferior to $^{18}$F-FDG as a PET tracer for general tumor diagnosis. Our preliminary results suggest rather selective uptake of $^{18}$F-FET in squamous cell carcinomas. Compared with $^{18}$F-FDG PET, $^{18}$F-FET PET may allow a better distinction between tumors and inflammatory tissues in patients with squamous cell carcinomas.

**Key Words:** *O*-(2-$^{18}$F-fluoroethyl)-L-tyrosine; $^{18}$F-FDG; peripheral tumors; squamous cell carcinomas; amino acids; PET

**J Nucl Med 2005; 46:411–416**

Received Jul. 3, 2004; revision accepted Oct. 21, 2004.

For correspondence or reprints contact: Dirk Pauleit, MD, Institute of Medicine, Research Center Jülich, P.O. Box 1913, 52425 Jülich, Germany.

E-mail: pauleit@web.de

Radiolabeled amino acids have proven to be useful tracers in nuclear medicine, especially for the diagnosis of brain tumors as well as for peripheral tumors, such as lymphomas (*1,2*). In the majority of studies, PET with [methyl-$^{11}$C]-L-methionine (MET) or [1-$^{11}$C]-L-tyrosine has been applied; however, because of the short physical half-life of the $^{11}$C label (20 min), the use of these tracers remains restricted to a few PET centers with a cyclotron on site. SPECT with L-3-$^{123}$I-iodo-α-methyltyrosine (IMT) has been shown to be an alternative for the investigation of cerebral gliomas (*1,3,4*); however, because of the poorer spatial resolution of SPECT, the diagnostic potential of the method remains inferior to that of PET.

In order to overcome the logistic disadvantages of $^{11}$C-labeled amino acids, several attempts have been undertaken to label amino acids with $^{18}$F (half-life, 110 min) (*5,6*). A very promising $^{18}$F-labeled amino acid is *O*-(2-$^{18}$F-fluoroethyl)-L-tyrosine ($^{18}$F-FET), which can be synthesized with high radiochemical yields, allowing large-scale production for clinical purposes (*7,8*). Although $^{18}$F-FET is not incorporated into proteins, uptake into mammalian cells is stereospecific and is mediated by sodium-independent transport via system L as well as sodium-dependent transport via a system similar to system $B^{0,+}$ (*9,10*). Initial clinical studies with $^{18}$F-FET PET in human brain tumors have shown results similar to those obtained with MET PET and IMT SPECT (*11,12*). A superior delineation of human solid gliomas by $^{18}$F-FET PET compared with MRI has been demonstrated by use of stereotactic biopsy samples as a reference (*13,14*). Furthermore, it has been shown in animal experiments that, compared with MET and 2-$^{18}$F-FDG ($^{18}$F-FDG),$^{18}$F-FET exhibits low uptake in nonneoplastic inflammatory cells and in inflammatory lymph nodes and therefore promises high specificity for the detection of tumor cells (*15,16*). The purpose of this study was to investigate the diagnostic potential of $^{18}$F-FET for a series of peripheral tumors.

## MATERIALS AND METHODS

### Patients

Forty-four consecutive patients believed to have malignant peripheral tumors participated in this study. Six patients were excluded from further analysis because a malignant tumor could not be verified. Of the remaining 38 patients (14 women and 24 men; mean ± SD age, 61 ± 13 y; age range, 30–81 y), 7 had colorectal cancer, 6 had pancreatic cancer, 9 had head–neck cancer, 4 had lymphomas, 3 had lung cancer, 3 had ovarian cancer, 4 had breast cancer, and 2 had prostatic cancer. Individual data for the patients are given in Table 1. The study was approved by university ethics committees and by federal authorities. All subjects gave written informed consent for participation in the study.

### Radiopharmaceuticals

The amino acid derivative $^{18}$F-FET was produced by anion-activated nucleophilic $^{18}$F-fluorination of *N*-trityl-*O*-(2-tosyloxyethyl)-L-tyrosine tert butyl ester and subsequent deprotection to yield a specific radioactivity of >200 GBq/μmol by optimization of a previously described method (*8*). The uncorrected yield was about 35%, and the radiochemical purity was >98%. The tracer was administered as an isotonic neutral solution.

$^{18}$F-FDG was synthesized as previously described (*17*). The average specific radioactivity was >200 GBq/μmol.

### PET

All patients fasted for at least 12 h before the PET studies. After intravenous injection of 370 MBq of $^{18}$F-FET, whole-body PET

**TABLE 1**
Patient Data, Histologic Diagnosis, and Staging by $^{18}$F-FDG PET and $^{18}$F-FET PET

| Patient | Age (y) | Sex | Primary tumor | Histologic diagnosis | Confirmation | Pretreatment | $^{18}$F-FDG staging* | No. of lesions | $^{18}$F-FET staging* | No. of lesions |
|---|---|---|---|---|---|---|---|---|---|---|
| 1 | 45 | F | Lymphoma | HG NHL | Surgery | Chemotherapy | II | 5 | (−) | 0 |
| 2 | 81 | M | Lymphoma | HG NHL | Biopsy | Chemotherapy | IV | >5 | (−) | 0 |
| 3 | 41 | M | Lymphoma | LG NHL | Biopsy | Chemotherapy | I | 1 | (−) | 0 |
| 4 | 39 | F | Lymphoma | LG NHL | Biopsy | Chemotherapy | IV | >5 | (−) | 0 |
| 5 | 48 | F | Colorectal | Adenoca. | Surgery | Chemotherapy | T(−) N0, M1 | >5 | T(−) N0, M0 | 0 |
| 6 | 67 | M | Colorectal | Adenoca. | Biopsy | None | T(+) N0, M0 | 1 | T(−) N0, M0 | 0 |
| 7 | 59 | M | Colorectal | Adenoca. | Surgery | Surgery/chemotherapy | T(−) N0, M1 | 2 | T(−) N0, M0 | 0 |
| 8 | 76 | M | Colorectal | Adenoca. | Surgery | Surgery | T(+) N0, M1 | >5 | T(−) N0, M0 | 0 |
| 9 | 50 | M | Colorectal | Adenoca. | Surgery | Surgery/chemotherapy | T(−) N0, M1 | 3 | T(−) N0, M0 | 0 |
| 10 | 77 | M | Colorectal | Adenoca. | Surgery | Surgery/chemotherapy | T(−) N0, M1 | 1 | T(−) N0, M0 | 0 |
| 11 | 48 | M | Colorectal | Adenoca. | Surgery | Surgery/chemotherapy | T(−) N0, M1 | 2 | T(−) N0, M0 | 0 |
| 12 | 69 | F | Pancreatic | Adenoca. | Surgery | Surgery/chemotherapy | T(−) N0, M1 | 2 | T(−) N0, M0 | 0 |
| 13 | 54 | M | Pancreatic | Adenoca. | Surgery | None | T(+) N0, M0 | 1 | T(−) N0, M0 | 0 |
| 14 | 56 | F | Pancreatic | Adenoca. | Biopsy | Chemotherapy | T(+) N0, M0 | 1 | T(−) N0, M0 | 0 |
| 15 | 62 | M | Pancreatic | Adenoca. | Biopsy | None | T(+) N1, M1 | >5 | T(−) N0, M0 | 0 |
| 16 | 57 | M | Pancreatic | Adenoca. | Biopsy | None | T(+) N1, M1 | >5 | T(−) N0, M0 | 0 |
| 17 | 76 | M | Pancreatic | Adenoca. | Surgery | None | T(+) N0, M0 | 1 | T(−) N0, M0 | 0 |
| 18 | 69 | M | Lung | SCC | Biopsy | None | T(+) N1, M1 | >5 | T(+) N1, M1 | >5 |
| 19 | 72 | F | Lung | SCC | Biopsy | None | T(+) N1, M1 | >5 | T(+) N1, M1 | >5 |
| 20 | 69 | M | Lung | Mixed CC | Biopsy | None | T(+) N0, M1 | 3 | T(−) N0, M0 | 0 |
| 21 | 52 | F | Ovarian | Adenoca. | Biopsy | None | T(−) N1, M1 | >5 | T(−) N0, M0 | 0 |
| 22 | 46 | F | Ovarian | Adenoca. | Surgery | Surgery | T(−) N0, M1 | 4 | T(−) N0, M0 | 0 |
| 23 | 63 | F | Ovarian | Adenoca. | Surgery | Surgery/chemotherapy | T(−) N1, M1 | >5 | T(−) N0, M0 | 0 |
| 24 | 81 | M | Prostatic | Adenoca. | Biopsy | Antiandrogen | T(+) N1, M1 | >5 | T(−) N0, M0 | 0 |
| 25 | 76 | M | Prostatic | Adenoca. | Biopsy | Antiandrogen | T(−) N0, M1 | 1 | T(−) N0, M0 | 0 |
| 26 | 76 | F | Breast | IDC | Surgery | None | T(+) N3, M1 | >5 | T(−) N0, M0 | 0 |
| 27 | 30 | F | Breast | IDC | Biopsy | None | T(+) N3, M0 | 3 | T(+) N3, M0 | 3 |
| 28 | 65 | F | Breast | IDC | Biopsy | None | T(+) N1, M0 | 2 | T(+) N1, M0 | 2 |
| 29 | 65 | F | Breast | IDC | Biopsy | None | T(+) N1, M0 | 2 | T(+) N1, M0 | 2 |
| 30 | 47 | M | Head–neck | SCC | Surgery | None | T(+) N2c, M0 | >5 | T(+) N2c, M0 | >5 |
| 31 | 41 | M | Head–neck | SCC | Surgery | None | T(+) N0, M1 | 3 | T(+) N0, M0 | 1 |
| 32 | 63 | M | Head–neck | SCC | Surgery | None | T(+) N2c, M0 | >5 | T(+) N2c, M0 | 3 |
| 33 | 68 | M | Head–neck | SCC | Surgery | Surgery | T(+) N0, M0 | 1 | T(+) N0, M0 | 1 |
| 34 | 73 | M | Head–neck | SCC | Surgery | Surgery | T(+) N0, M1 | 2 | T(+) N0, M0 | 1 |
| 35 | 73 | M | Head–neck | Adenoca. | Surgery | None | T(−) N0, M0 | 0 | T(−) N0, M0 | 0 |
| 36 | 59 | M | Head–neck | SCC | Surgery | None | T(+) N1, M0 | 2 | T(+) M0, M0 | 1 |
| 37 | 61 | M | Head–neck | SCC | Biopsy | None | T(+) N1, M1 | 3 | T(+) N0, M0 | 1 |
| 38 | 73 | F | Head–neck | SCC | Biopsy | None | T(+) N1, M1 | 4 | T(+) N0, M0 | 1 |

*Clinical staging was done according to International Union Against Cancer with modification of T status as follows: T(+) = tumor present; T(−) = tumor absent. HG NHL = high-grade non-Hodgkin's lymphoma; LG NHL = low-grade non-Hodgkin's lymphoma; adenoca. = adenocarcinoma; SCC = squamous cell carcinoma; mixed CC = mixed-cell carcinoma; IDC = infiltrating duct carcinoma of breast.

scans were obtained starting at 1 h after injection. The duration of the whole-body PET scans ranged from 50 to 100 min, depending on the number of bed positions acquired. All patients underwent comparative investigations after intravenous injection of 370 MBq of $^{18}$F-FDG within 1 wk by use of the same scanning protocol. Blood glucose levels were checked before $^{18}$F-FDG injection to ensure that they were <130 mg/dL.

The studies were performed with a CTI ECAT Exact HR+ scanner (optimum full width at half maximum, 4.5 mm; 15-cm transaxial field of view). For attenuation correction, transmission scans with 3 $^{68}$Ge/$^{68}$Ga rotating line sources were used. After correction for random and scattered coincidences, dead time, and decay, image data were obtained by iterative reconstruction. Data were reconstructed with the manufacturer-supplied ordered-subset expectation maximization algorithm including attenuation correction (*18*).

### Data Analysis

The data were evaluated in 2 separate sessions. In the first session, $^{18}$F-FDG and $^{18}$F-FET PET scans of all patients were visually analyzed for the presence of increased tracer uptake by 2 experienced nuclear medicine physicians with knowledge of clinical data. $^{18}$F-FET PET and $^{18}$F-FDG PET images were coregistered (MPI tool 3.28; ATV) (*19*) before evaluation to enable a direct comparison of the anatomic regions. A standardized uptake value (SUV) threshold of >2.5 was used for increased $^{18}$F-FDG uptake as reported previously (*20*). The cutoff for increased $^{18}$F-FET uptake (SUV > 2.0) was derived from whole-body distribution studies (*21*). The numbers of regions with abnormal tracer uptake indicative of a tumor were documented by consensus (1 to 5 or >5). Scan findings were staged according to the International Union Against Cancer (*22*) with modification of the T status as follows: T(+) for primary tumor present and T(−) for primary tumor absent. A quantitative comparison of $^{18}$F-FDG and $^{18}$F-FET in all patients was not performed because no pathologic $^{18}$F-FET accumulation could be detected in the majority of patients. $^{18}$F-FDG PET scans were used as a reference because histologic confirmation was not available for all lesions.

In the second session, quantitative data analysis was done for a subgroup of patients with head–neck carcinomas that demonstrated increased uptake of $^{18}$F-FET, in contrast to most other tumor types. For these patients, analyses of correlations with CT, clinical findings, and histologic results were performed.

On the coregistered CT, $^{18}$F-FDG PET, and $^{18}$F-FET PET images, regions with increased tracer uptake were identified by computed analysis (MPI tool) with the above-mentioned thresholds. Regions of interest (ROIs) were drawn manually over the corresponding anatomic structures on the coregistered CT scans. Identical ROIs were transferred to the $^{18}$F-FDG and $^{18}$F-FET images for quantification to enable the comparison of $^{18}$F-FDG uptake and $^{18}$F-FET uptake in the same anatomic structure. SUVs for $^{18}$F-FET uptake and $^{18}$F-FDG uptake were calculated by dividing the mean radioactivity (kBq/mL) of the ROIs by the radioactivity injected per gram of body weight in the corresponding PET scans. For comparison of the SUVs for $^{18}$F-FET uptake and $^{18}$F-FDG uptake, the nonparametric Mann–Whitney *U* test was used. Differences were considered significant at a $P$ level of <0.05.

## RESULTS

### $^{18}$F-FET PET and $^{18}$F-FDG PET in All Patients

Similar results for staging by $^{18}$F-FDG PET and $^{18}$F-FET PET according to the International Union Against Cancer were found for 8 of 38 patients, and discordant results were found for 30 of 38 patients.

$^{18}$F-FDG PET showed increased $^{18}$F-FDG uptake in 37 of 38 patients, and only 1 head–neck mucoid adenocarcinoma (patient 35) showed no increased uptake of $^{18}$F-FDG.

In contrast, $^{18}$F-FET PET was positive in only 13 of 38 patients (34%); these included 2 of 3 patients with lung carcinomas, 3 of 4 patients with breast carcinomas, and 8 of 9 patients with head–neck carcinomas. Increased $^{18}$F-FET uptake could not be identified in any of the patients with lymphomas, colorectal carcinomas, pancreatic carcinomas, ovarian carcinomas, or prostatic carcinomas (Fig. 1). Interestingly, all squamous cell carcinomas were found to be $^{18}$F-FET–positive tumors (8 head–neck carcinomas and 2 lung carcinomas), whereas most adenocarcinomas were found to be $^{18}$F-FET–negative tumors (in only 3 patients with infiltrating duct carcinomas of the breasts was increased $^{18}$F-FET uptake seen).

All lesions with increased $^{18}$F-FET uptake exhibited concordant $^{18}$F-FDG accumulation, and no additional lesion was identified by $^{18}$F-FET PET but not by $^{18}$F-FDG PET. Detailed data for each patient are given in Table 1.

### $^{18}$F-FET PET and $^{18}$F-FDG PET in Patients with Head–Neck Carcinomas

Among patients with head–neck carcinomas, 8 of 9 patients were found to have squamous cell carcinomas and 1 of 9 patients was found to have an adenocarcinoma by

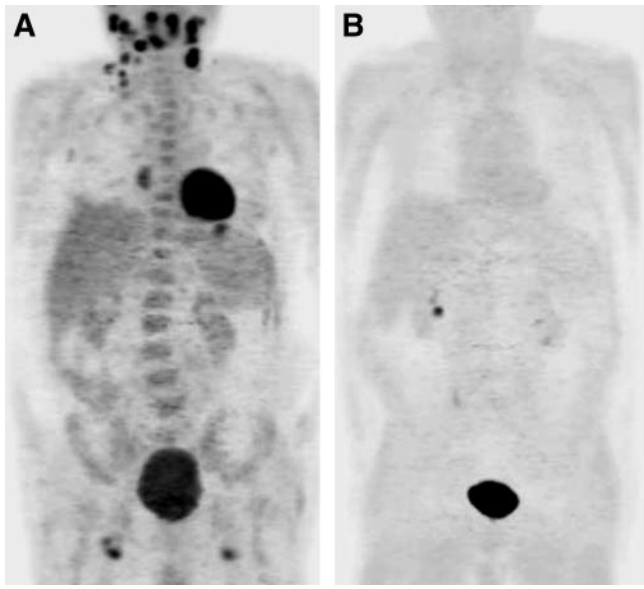


**FIGURE 1.** $^{18}$F-FDG PET (A) and $^{18}$F-FET PET (B) of 81-y-old man (patient 2) with high-grade lymphoma (non-Hodgkin's lymphoma). $^{18}$F-FDG shows high uptake in multiple lymph nodes, whereas $^{18}$F-FET uptake is negative in all lymph nodes.

subsequent histologic analyses. The adenocarcinoma was missed by both $^{18}$F-FDG PET and $^{18}$F-FET PET.

On $^{18}$F-FDG PET scans of patients with head–neck carcinomas, 31 lesions showing increased $^{18}$F-FDG uptake (SUV $\geq$2.5) were identified. Of the 31 lesions, 16 were tumorous and 15 were nontumorous, according to CT, clinical findings, and histologic results. On $^{18}$F-FET PET scans, 15 of the 16 tumorous lesions exhibited increased $^{18}$F-FET uptake and were correctly identified (Fig. 2); only 1 lymph node metastasis was missed on $^{18}$F-FET PET scans (SUV for $^{18}$F-FDG uptake, 3.3; SUV for $^{18}$F-FET uptake, 1.7). Among the nontumorous lesions, $^{18}$F-FET PET was superior to $^{18}$F-FDG PET; increased $^{18}$F-FET uptake was seen in only 2 of 15 lesions, and normal uptake was seen in 13 of 15 lesions (Fig. 3).

The mean $\pm$ SD SUVs for $^{18}$F-FET uptake were significantly lower ($P < 0.001$) in tumorous (3.9 $\pm$ 2.1) and nontumorous (1.5 $\pm$ 0.4) lesions than the SUVs of 10.4 $\pm$ 6.3 and 3.7 $\pm$ 0.9, respectively, for $^{18}$F-FDG uptake.

## DISCUSSION

In this study, we investigated the diagnostic potential of $^{18}$F-FET for the imaging of peripheral tumors. PET studies with $^{18}$F-FET for brain tumors have demonstrated high diagnostic accuracy (*11–14*), and experimental studies have shown a higher specificity of $^{18}$F-FET than of $^{8}$F-FDG and MET in the differentiation of inflammatory tissues from malignancies (*15,16*). Also, experimental colon carcinomas in mice exhibited increased $^{18}$F-FET uptake (*9*), but to date no clinical data are available concerning the behavior of $^{18}$F-FET in human tumors outside the brain.

Surprisingly, we found no increased uptake of $^{18}$F-FET in the majority of tumors, especially in lymphomas and most adenocarcinomas, in contrast to the results obtained with other tyrosine derivatives, such as $^{11}$C-L-tyrosine (*23*), 2-$^{18}$F-fluoro-L-tyrosine (*20*), L-3-$^{18}$F-fluoro-α-tyrosine (*24*), and IMT (*25*). Interestingly, all squamous cell carcinomas were found to be $^{18}$F-FET–positive tumors, whereas most adenocarcinomas were found to be $^{18}$F-FET–negative tumors.

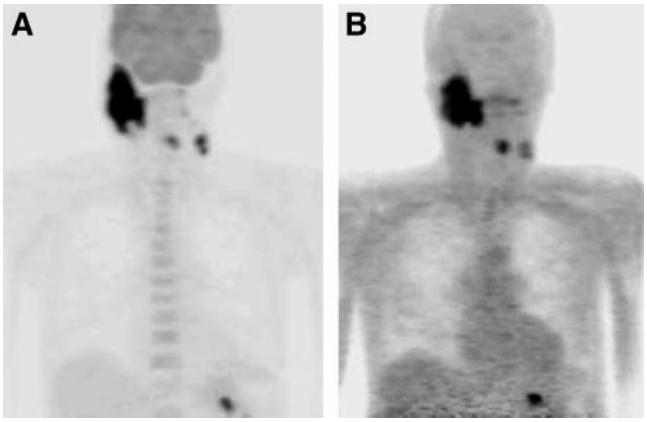


**FIGURE 2.** $^{18}$F-FDG PET (A) and $^{18}$F-FET PET (B) of 63-y-old man (patient 32) with head–neck carcinoma (squamous cell carcinoma). Primary tumor and lymph node metastases are positive for both $^{18}$F-FDG and $^{18}$F-FET.

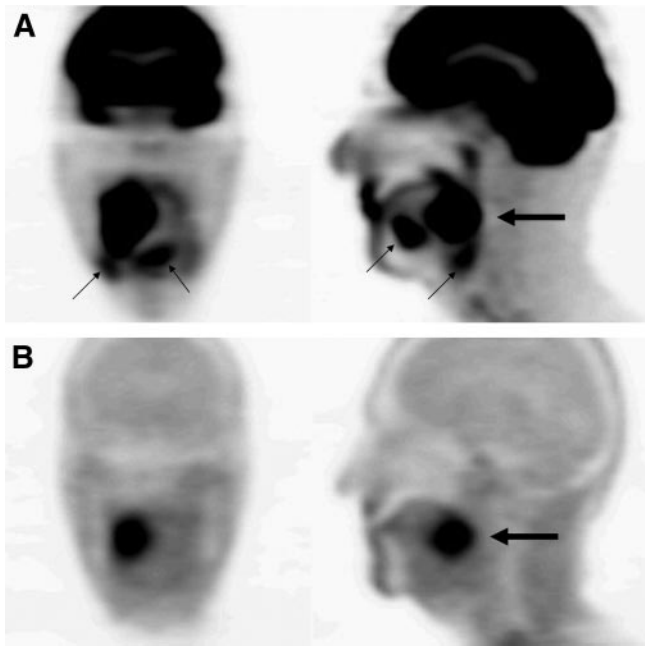


**FIGURE 3.** $^{18}$F-FDG PET (A) and $^{18}$F-FET PET (B) of 61-y-old man with cancer of tongue (squamous cell carcinoma). Increased $^{18}$F-FDG uptake was noted in tumor (large arrow), and additional uptake was demonstrated in inflammatory tissues (small arrows). Increased $^{18}$F-FET uptake was noted only in tumor (large arrow).

The tumor-to-background contrast was significantly lower in PET scans with $^{18}$F-FET than in those with $^{18}$F-FDG, and some smaller lesions may have been missed in the $^{18}$F-FET PET studies because of the partial-volume effect. All of the primary tumors and the majority of the lymph node metastases, however, were large enough to be detectable by PET even in the presence of low $^{18}$F-FET uptake (Fig. 1).

We suggest that the absence of tracer uptake in most peripheral tumors is caused by different transport characteristics of $^{18}$F-FET and other tyrosine derivatives and is not attributable to the fact that $^{18}$F-FET, unlike $^{11}$C-L-tyrosine and 2-$^{18}$F-fluoro-L-tyrosine, is not incorporated into proteins (*7*). Experiments with mice demonstrated that the inhibition of protein synthesis did not influence the uptake of MET in tumors and brains (*26*), suggesting that alterations in amino acid transport rather than increased protein synthesis caused increased uptake in tumors. Concordantly, a PET study with 2-$^{18}$F-fluoro-L-tyrosine and kinetic modeling showed that the difference in uptake between tumors and normal tissues was attributable to an increase in tracer transport whereas binding to the metabolic compartment was not altered or even decreased in tumors (*27*).

Data on the transport characteristics for $^{18}$F-FET are still limited. Compared with the D-isomer, L-$^{18}$F-FET showed

24-fold-higher uptake in the brains of nude mice, indicating stereoselective transport (*7*). An approximate 70% reduction in $^{18}$F-FET transport was observed in SW707 colon carcinoma cells with the amino acid analog 2-aminobicyclo-(2,2,1)-heptane-2-carboxylic acid (BCH). Although BCH is often regarded as a specific inhibitor of system L amino acid transport, this scenario is only true when transport assays are performed in the absence of $Na^+$. Under physiologic conditions, BCH also inhibits $Na^+$-dependent general amino acid transport via system $B^{0,+}$ (*28*) and system $B^0$ (*29*). In keeping with this notion, we found that the transport of $^{18}$F-FET in F98 rat glioma cells consisted of $Na^+$-dependent activity of approximately 70% and $Na^+$-independent activity of approximately 30% (*2,10*) and that both activities were sensitive to inhibition by BCH. As a result of our experiments, we suggest that $Na^+$-independent $^{18}$F-FET transport occurs via system L and that $Na^+$-dependent activity occurs via system $B^{0,+}$. The transport of $^{18}$F-FET in F98 glioma cells was also inhibited by serine, which is a substrate of system L, system $B^{0,+}$, and system $B^0$ amino acid transport.

Amino acid transport via system L is currently thought to be mediated by 3 different proteins, namely, LAT1, LAT2, and LAT3 (*30–33*). The first 2 are composed of a light chain (LAT1 and LAT2) covalently linked to a heavy glycoprotein chain (4F2hc). Both subunits are necessary for functional expression. In contrast to the LAT1 and LAT2 subtypes, LAT3 does not require 4F2hc for functional expression. Although 4F2hc–LAT1 is found quite ubiquitously and is highly expressed in proliferating tissues and in tumors, 4F2hc–LAT2 is found only in tissues containing epithelial barriers (*34*). LAT3 has a rather restricted distribution and is found in liver, pancreas, and skeletal muscle.

As mentioned above, $Na^+$-dependent transport of $^{18}$F-FET is likely to be mediated by amino acid transport via system $B^{0,+}$ and system $B^0$. The molecular correlates of these transporters are members of the SLC6 family encoded by cDNAs $ATB^{0,+}$ (*28*) and $B^0AT1$ (*29*). Both transporters are able to accumulate substrates several thousandfold.

Expression experiments with *Xenopus* oocytes showed that the radioiodinated tyrosine derivative IMT was selectively transported via the human LAT1 (hLAT1) subtype of system L, whereas the natural parent tyrosine was transported via both hLAT1 and hLAT2 (*35*). Recently, it was demonstrated by transstimulation experiments with *Xenopus laevis* oocytes after the expression of 4F2hc–LAT1 that $^{18}$F-FET influx via LAT1 was poor (*36*).

Several observations suggest that $^{18}$F-FET may be selectively transported via hLAT2. First, $^{18}$F-FET transport in F98 glioma cells is shared by serine (*10*), which is a substrate of hLAT2 but not of hLAT1. Second, $^{18}$F-FET shows no uptake in inflammatory tissues (*15,16*), in which hLAT2 is not expressed (*37*). Third, $^{18}$F-FET shows some retention in muscles (*21*), in which hLAT2 is expressed (*38*). Fourth, $^{18}$F-FET transport can be inhibited by BCH (*10*), which inhibits both hLAT1 transport and hLAT2 transport (*29*). In this study, $^{18}$F-FET did not accumulate in most adenocarcinomas, but we found increased uptake in all squamous cell carcinomas. As mentioned above, human 4F2hc (h4F2hc)–hLAT2 is highly expressed in tissues containing epithelial barriers (*34*), in agreement with the hypothesis of selective transport of $^{18}$F-FET via h4F2hc–hLAT2. The exact mechanisms of $^{18}$F-FET transport remain to be elucidated. Beside uptake via amino acid exchange transporters, such as hLAT2, actively accumulating systems, such as $B^{0,+}$ and $B^0$, must be considered. Further studies are required to discriminate among these possibilities.

From the clinical point of view, it is important to note that all $^{18}$F-FET–positive lesions in patients with squamous cell carcinomas also showed increased uptake of $^{18}$F-FDG and that the SUV for $^{18}$F-FDG uptake was significantly higher than that for $^{18}$F-FET uptake. No additional lesion was identified by $^{18}$F-FET PET but not by $^{18}$F-FDG PET. Thus, $^{18}$F-FET PET is not able to improve sensitivity for the detection of squamous cell carcinomas but may allow better distinction between tumors and inflammatory tissues. This finding must be confirmed with a larger series of patients. In head–neck carcinomas, for example, it is known that $^{18}$F-FDG has a low specificity (*39,40*).

Although $^{18}$F-FET is inferior to $^{18}$F-FDG for general tumor diagnosis, it is important to note that some amino acids exhibit higher selectivity for certain amino acid transporter subtypes after being labeled with iodine or fluorine than do their natural parents. This property not only may improve specificity in the differentiation of tumors and inflammatory tissues but also may indicate a possible use in the pretherapeutic assessment of antitumor drug selectivity. For instance, IMT and the phenylalanine mustard melphalan are transported by LAT1–4F2hc and accumulate in cancer cells (*37,41*).

## CONCLUSION

$^{18}$F-FET is inferior to $^{18}$F-FDG as a PET tracer for general tumor diagnosis. Our preliminary results suggest a rather selective uptake of $^{18}$F-FET in squamous cell carcinomas. Compared with $^{18}$F-FDG PET, $^{18}$F-FET PET appears to allow better distinction between tumors and inflammatory tissues in patients with squamous cell carcinomas.

## ACKNOWLEDGMENTS

The authors thank Elisabeth Theelen and Suzanne Schaden for assistance in patient studies and data analysis and Bettina Palm, Erika Wabbals, and Silke Grafmüller for technical assistance in the radiosynthesis of $^{18}$F-FET.

## REFERENCES

1. Jager PL, Vaalburg W, Pruim J, de Vries EG, Langen KJ, Piers DA. Radiolabeled amino acids: basic aspects and clinical applications in oncology. *J Nucl Med*. 2001;42:432–445.
2. Langen KJ. Amino acid transport studies in brain tumors. In: Feinendegen LE, Shreeve WW, Eckelman WC, Bahk YW, Wagner HN Jr, eds. *Molecular Nuclear Medicine: The Challenge of Genomics and Proteomics to Clinical Practice*. Berlin, Germany: Springer-Verlag; 2003:477–485.

3. Weckesser M, Schmidt D, Matheja P, Coenen HH, Langen KJ. The role of L-3-I-123-iodine-alpha-methyltyrosine SPECT in cerebral gliomas. *Nuklearmedizin*. 2000;39:233–240.
4. Langen KJ, Pauleit D, Coenen HH. [$^{123}$I]Iodo-α-methyl-L-tyrosine: uptake mechanisms and clinical applications. *Nucl Med Biol*. 2002;29:625–631.
5. Coenen HH. Biochemistry and evaluation of fluoroamino acids. In: Mazoyer BM, Heiss WD, Comar D, eds. *PET Studies on Amino Acid Metabolism and Protein Synthesis*. Dordrecht, The Netherlands: Kluwer Academic Publishers; 1993:109–129.
6. Laverman P, Boerman OC, Corstens FH, et al. Fluorinated amino acids for tumour imaging with positron emission tomography. *Eur J Nucl Med Mol Imaging*. 2002;29:681–690.
7. Wester HJ, Herz M, Weber W, et al. Synthesis and radiopharmacology of *O*-(2-[$^{18}$F]fluoroethyl)-L-tyrosine for tumor imaging. *J Nucl Med*. 1999;40:205–212.
8. Hamacher K, Coenen HH. Efficient routine production of the $^{18}$F-labelled amino acid *O*-2-$^{18}$F fluoroethyl-L-tyrosine. *Appl Radiat Isot*. 2002;57:853–856.
9. Heiss P, Mayer S, Herz M, Wester HJ, Schwaiger M, Senekowitsch-Schmidtke R. Investigation of transport mechanism and uptake kinetics of *O*-(2-[$^{18}$F]fluoroethyl)-L-tyrosine in vitro and in vivo. *J Nucl Med*. 1999;40:1367–1373.
10. Langen KJ, Jarosch M, Mühlensiepen H, et al. Comparison of fluorotyrosines and methionine uptake in F98 rat gliomas. *Nucl Med Biol*. 2003;30:501–508.
11. Weber WA, Wester HJ, Grou AL, et al. *O*-(2-[$^{18}$ F]Fluoroethyl)-L-tyrosine and L-[methyl-$^{11}$C]methionine uptake in brain tumours: initial results of a comparative study. *Eur J Nucl Med Mol Imaging*. 2000;27:542–549.
12. Pauleit D, Floeth F, Tellmann L, et al. Comparison of *O*-(2-$^{18}$F-fluoroethyl)-L-tyrosine PET and 3-$^{123}$I-iodo-α-methyl-L-tyrosine SPECT in brain tumors. *J Nucl Med*. 2004;45:374–381.
13. Messing-Jünger AM, Floeth FW, Pauleit D, et al. Multimodal target point assessment for stereotactic biopsy in children with diffuse bithalamic astrocytomas. *Child's Nerv Syst*. 2002;18:445–449.
14. Pauleit D, Langen KJ, Floeth F, et al. Improved delineation of the tumor extension using *O*-(2-$^{18}$F-fluoroethyl)-L-tyrosine PET compared with MRI in cerebral gliomas [abstract]. *J Nucl Med*. 2002;43(suppl):112P.
15. Kaim AH, Weber B, Kurrer MO, et al. $^{18}$F-FDG and $^{18}$F-FET uptake in experimental soft tissue infection. *Eur J Nucl Med Mol Imaging*. 2002;29:648–654.
16. Rau FC, Weber WA, Wester HJ, et al. O-(2-[$^{18}$F]Fluoroethyl)-L-tyrosine (FET): a tracer for differentiation of tumour from inflammation in murine lymph nodes. *Eur J Nucl Med Mol Imaging*. 2002;29:1039–1046.
17. Hamacher K, Coenen HH, Stöcklin G. Efficient stereospecific synthesis of no-carrier-added 2-[$^{18}$F]-fluoro-2-deoxy-D-glucose using aminopolyether supported nucleophilic substitution. *J Nucl Med*. 1986;27:235–238.
18. Liu X, Comtat C, Michel C, Kinahan P, Defrise M, Townsend D. Comparison of 3-D reconstruction with 3D-OSEM and with FORE+OSEM for PET. *IEEE Trans Med Imaging*. 2001;20:804–814.
19. Pietrzyk U, Herholz K, Heiss WD. Three-dimensional alignment of functional and morphological tomograms. *J Comput Assist Tomogr*. 1990;14:51–59.
20. Hustinx R, Lemaire C, Jerusalem G, et al. Whole-body tumor imaging using PET and 2-$^{18}$F-fluoro-L-tyrosine: preliminary evaluation and comparison with $^{18}$F-FDG. *J Nucl Med*. 2003;44:533–539.
21. Pauleit D, Floeth F, Herzog H, et al. Whole-body distribution and dosimetry of *O*-(2-$^{18}$F-fluoroethyl)-L-tyrosine (FET). *Eur J Nucl Med Mol Imaging*. 2003;30:519–524.
22. Sobin LH, Wittekind Ch, eds. *TNM Classification of Malignant Tumours*. 6th ed. Indianapolis, IN: Wiley press; 2002.
23. Kole AC, Pruim J, Nieweg OE, et al. PET with L-[1-carbon-11]-tyrosine to visualize tumors and measure protein synthesis rates. *J Nucl Med*. 1997;38:191–195.
24. Inoue T, Koyama K, Oriuchi N, et al. Detection of malignant tumors: whole-body PET with fluorine-18 alpha-methyltyrosine versus FDG—preliminary study. *Radiology*. 2001;220:54–62.
25. Jager PL, Franssen EJ, Kool W, et al. Feasibility of tumor imaging using L-3-[iodine-123]-iodo-alpha-methyl-tyrosine in extracranial tumors. *J Nucl Med*. 1998;39:1736–1743.
26. Ishiwata K, Kubota K, Murakami M, et al. Reevaluation of amino acid PET studies: can the protein synthesis rates in brain and tumor tissues be measured in vivo? *J Nucl Med*. 1993;34:1936–1943.
27. Wienhard K, Herholz K, Coenen HH, et al. Increased amino acid transport into brain tumors measured by PET of L-(2-$^{18}$F)fluorotyrosine. *J Nucl Med*. 1991;32:1338–1346.
28. Sloan JL, Mager S. Cloning and functional expression of a human Na(+) and Cl(−)-dependent neutral and cationic amino acid transporter B(0+). *J Biol Chem*. 1999;274:23740–23745.
29. Broer A, Klingel K, Kowalczuk S, Rasko JE, Cavanaugh J, Broer S. Molecular cloning of mouse amino acid transport system B0, a neutral amino acid transporter related to Hartnup disorder. *J Biol Chem*. 2004;279:24467–24476.
30. Kanai Y, Segawa H, Miyamoto K, Uchino H, Takeda E, Endou H. Expression cloning and characterization of a transporter for large neutral amino acids activated by the heavy chain of 4F2 antigen (CD98). *J Biol Chem*. 1998;273:23629–23632.
31. Pineda M, Fernandez E, Torrents D, et al. Identification of a membrane protein, LAT-2, that co-expresses with 4F2 heavy chain, an L-type amino acid transport activity with broad specificity for small and large zwitterionic amino acids. *J Biol Chem*. 1999;274:19738–19744.
32. Babu E, Kanai Y, Chairoungdua A, et al. Identification of a novel system L amino acid transporter structurally distinct from heterodimeric amino acid transporters. *J Biol Chem*. 2003;278:43838–43845.
33. Mastroberardino L, Spindler B, Pfeiffer R, et al. Amino-acid transport by heterodimers of 4F2hc/CD98 and members of a permease family. *Nature*. 1998;395:288–291.
34. Verrey F. System L: heteromeric exchangers of large, neutral amino acids involved in directional transport. *Pflugers Arch*. 2003;445:529–533.
35. Shikano N, Kanai Y, Kawai K, et al. Isoform selectivity of 3-$^{125}$I-iodo-alpha-methyl-L-tyrosine membrane transport in human L-type amino acid transporters. *J Nucl Med*. 2003;44:244–246.
36. Lahoutte T, Caveliers V, Camargo SM, et al. SPECT and PET amino acid tracer influx via system L (h4F2hc-hLAT1) and its transstimulation. *J Nucl Med*. 2004;45:1591–1596.
37. Rau FC, Philippi H, Rubio-Aliaga I, et al. Identification of subtypes of amino acid transporters in human tumor and inflammatory cells by reverse transcription-polymerase chain reaction [abstract]. *J Nucl Med*. 2002;43(suppl):24P.
38. Verrey F, Closs EI, Wagner CA, Palacin M, Endou H, Kanai Y. CATs and HATs: the SLC7 family of amino acid transporters. *Pflugers Arch*. 2004;447:532–542.
39. Greven KM, Keyes JW Jr, Williams DW III, McGuirt WF, Joyce WT III. Occult primary tumors of the head and neck: lack of benefit from positron emission tomography imaging with 2-[F-18]fluoro-2-deoxy-D-glucose. *Cancer*. 1999;86:114–118.
40. Kunkel M, Forster GJ, Reichert TE, et al. Detection of recurrent oral squamous cell carcinoma by [$^{18}$F]-2-fluorodeoxyglucose-positron emission tomography: implications for prognosis and patient management. *Cancer*. 2003;98:2257–2265.
41. Uchino H, Kanai Y, Kim do K, et al. Transport of amino acid-related compounds mediated by L-type amino acid transporter 1 (LAT1): insights into the mechanisms of substrate recognition. *Mol Pharmacol*. 2002;61:729–737.